

1-1-1993

Theoretical study of interacting low dimensional electron systems

Jianzhong Zheng

University of Nevada, Las Vegas

Follow this and additional works at: <https://digitalscholarship.unlv.edu/rtds>

Repository Citation

Zheng, Jianzhong, "Theoretical study of interacting low dimensional electron systems" (1993). *UNLV Retrospective Theses & Dissertations*. 276.

<http://dx.doi.org/10.25669/hsjs-6ti2>

This Thesis is protected by copyright and/or related rights. It has been brought to you by Digital Scholarship@UNLV with permission from the rights-holder(s). You are free to use this Thesis in any way that is permitted by the copyright and related rights legislation that applies to your use. For other uses you need to obtain permission from the rights-holder(s) directly, unless additional rights are indicated by a Creative Commons license in the record and/or on the work itself.

This Thesis has been accepted for inclusion in UNLV Retrospective Theses & Dissertations by an authorized administrator of Digital Scholarship@UNLV. For more information, please contact digitalscholarship@unlv.edu.

INFORMATION TO USERS

This manuscript has been reproduced from the microfilm master. UMI films the text directly from the original or copy submitted. Thus, some thesis and dissertation copies are in typewriter face, while others may be from any type of computer printer.

The quality of this reproduction is dependent upon the quality of the copy submitted. Broken or indistinct print, colored or poor quality illustrations and photographs, print bleedthrough, substandard margins, and improper alignment can adversely affect reproduction.

In the unlikely event that the author did not send UMI a complete manuscript and there are missing pages, these will be noted. Also, if unauthorized copyright material had to be removed, a note will indicate the deletion.

Oversize materials (e.g., maps, drawings, charts) are reproduced by sectioning the original, beginning at the upper left-hand corner and continuing from left to right in equal sections with small overlaps. Each original is also photographed in one exposure and is included in reduced form at the back of the book.

Photographs included in the original manuscript have been reproduced xerographically in this copy. Higher quality 6" x 9" black and white photographic prints are available for any photographs or illustrations appearing in this copy for an additional charge. Contact UMI directly to order.

U·M·I

University Microfilms International
A Bell & Howell Information Company
300 North Zeeb Road, Ann Arbor, MI 48106-1346 USA
313/761-4700 800/521-0600

Order Number 1352570

**Theoretical study of interacting low dimensional electron
systems**

Zheng, Jianzhong, M.S.

University of Nevada, Las Vegas, 1993

U·M·I

**300 N. Zeeb Rd.
Ann Arbor, MI 48106**

Theoretical Study of Interacting Low Dimensional Electron Systems

by

Jianzhong Zheng

A thesis submitted in partial fulfillment
of the requirements for the degree of

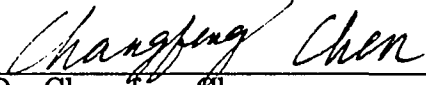
Master of Science


in

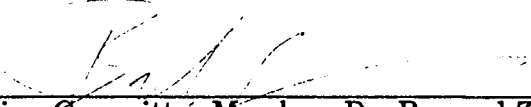
Physics

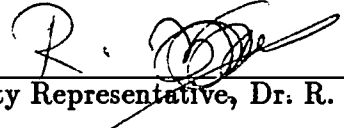
**Department of Physics
University of Nevada, Las Vegas
May 1993**

The Thesis of Jianzhong Zheng for the degree of Master of Science in Physics
is approved.

 4/22/93
Chairperson, Dr. Changfeng Chen

 4/22/93
Examining Committee Member, Dr. Tao Pang

 4/22/93
Examining Committee Member, Dr. Bernard Zygelman

 4/22/93
Graduate Faculty Representative, Dr. R. Venkatasubramanian

Dean of the Graduate College, Dr. Ronald W. Smith

University of Nevada, Las Vegas

May 1993

ABSTRACT

This thesis addresses the question of a strongly interacting many-body problem: the Hubbard model on one- and two-dimensional lattices. The technique employed is the small-cluster method wherein the full many-body Hamiltonian for finite clusters with periodic boundary conditions (PBC's) is solved exactly. We first apply this technique to an extended one-dimensional chain and a two-dimensional square-lattice Hubbard model. We then construct a two-dimensional overlayer/substrate Hubbard model with first- and second-nearest-neighbor hopping, on-site and nearest-neighbor interactions, and overlayer-site orbital energy. The ground-state properties are investigated and discussed in a many-body picture.

TABLE OF CONTENTS

ABSTRACT	iii
LIST OF FIGURES	vi
LIST OF TABLES	vii
ACKNOWLEDGEMENTS	ix
CHAPTER I INTRODUCTION	1
CHAPTER II THE HUBBARD HUMILTONIAN.....	6
CHAPTER III EXACT DIAGONALIZATION METHOD.....	9
III.1 Small Cluster Approach.....	9
III.2 Symmetry Analysis.....	10
A. Number Operator.....	12
B. Space Group Symmetry.....	12
C. Spin Symmetry.....	16
CHAPTER IV APPLICATIONS	19

IV.1 An Extended One – dimensional	
Hubbard Model.....	19
IV.2 A Two – dimensional Square Lattice Cluster	
Hubbard Model.....	32
IV.3 An Overlayer System.....	47
CHAPTER V CONCLUSIONS	56
BIBLIOGRAPHY	58

LIST OF FIGURES

FIGURE 1. An extended one-dimensional cluster.....	20
FIGURE 2. A four-site square lattice cluster.....	33
FIGURE 3. An eight-site overlayer/substrate cluster.....	48

LIST OF TABLES

Table 4.1.1. Degeneracy of the various representations.....	22
Table 4.1.2. The character table for the one-dimensional cluster.....	22
Table 4.1.3. The Hamiltonian matrix for $^1\Gamma$ symmetry.....	26
Table 4.1.4. The Hamiltonian matrix for 1X symmetry.....	27
Table 4.1.5. The Hamiltonian matrix for 1A symmetry.....	28
Table 4.1.6. The Hamiltonian matrix for $^3\Gamma$ symmetry.....	29
Table 4.1.7. The Hamiltonian matrix for 3X symmetry.....	29
Table 4.1.8. The Hamiltonian matrix for 3A symmetry.....	30
Table 4.1.9. The Multiplicity of the matrices for the various representations.....	31
Table 4.1.10. The 28 energy levels in the limit $U=K=0$	32
Table 4.1.11. The 28 energy levels in the limit $t=0$	32
Table 4.2.1. Neighbor structure for the four-site square lattice cluster.....	35
Table 4.2.2. Character table for the space group of the four-site cluster on the square lattice.....	36

Table 4.2.3. The mapping between the space-group and the point-group notations.....	37
Table 4.2.4. Reduced character table for four-site square cluster lattice	37
Table 4.2.5. Sizes of the Hamiltonian matrix blocks of spin and various spatial representations.....	38
Table 4.2.6. The Hamiltonian matrix for $^1\Gamma_1$ symmetry.....	40
Table 4.2.7. The Hamiltonian matrix for 1M_1 symmetry.....	41
Table 4.2.8. The Hamiltonian matrix for 1M_2 symmetry.....	42
Table 4.2.9. The Hamiltonian matrix for 1X symmetry.....	42
Table 4.2.10. The Hamiltonian matrix for $^3\Gamma_1$ symmetry.....	43
Table 4.2.11. The Hamiltonian matrix for $^3\Gamma_2$ symmetry.....	44
Table 4.2.12. The Hamiltonian matrix for 3M_1 symmetry.....	44
Table 4.2.13. The Hamiltonian matrix for 3X_1 symmetry.....	45
Table 4.3.1. Neighbor structure for the eight-site square lattice cluster.....	47
Table 4.3.2. Sizes of the Hamiltonian matrix blocks of spin and various spatial representations.....	50
Table 4.3.3. The character table for the overlayer system.....	51

ACKNOWLEDGEMENTS

I would like to express my special thanks to Dr. Changfeng Chen, under whose direction this work was carried out. As the sheer size of this undertaking began to make itself known, his critical judgement, continuing encouragement and warm-hearted instructions were greatly appreciated.

I would like to thank Dr. T. Pang, Dr. B. Zygelman and Dr. R. Venkatasubramanian for many valuable advices on this thesis.

I would like to acknowledge Cray Research Inc., and the Graduate College and the Physics Department of University of Nevada, Las Vegas, under whose sponsorship this work was done. I would also like to acknowledge the programming assistance by Mr. John Kilburg.

Finally, it is a great pleasure to thank Mr. Changshi Wu for his technique help in improving the presentation.

CHAPTER I

INTRODUCTION

The Hubbard model¹ has become, since its introduction in 1963, the prototype of a system of fermions with short-range interactions. It has been used to study a great variety of many-body effects in metals, of which ferromagnetism, antiferromagnetism, metal-insulator transitions, spin-density waves, and charge-density waves and high-temperature superconductivity are the most common examples¹⁻⁶.

The model has been applied to a variety of lattices — one, two, and three dimensional^{2,3,7-10} — and to small clusters^{11,12}. Due to the many-body nature of the model, exact solutions only exist in one dimension⁷. Analytically, there are many approximate solutions¹³⁻¹⁸ but unfortunately most of them are uncontrolled. Numerically, quantum Monte Carlo simulations have provided considerable insight into properties of the Hubbard model, especially in the half-filled band¹⁹. However, the so-called "negative sign" problem at non-half-filled band prevents it from providing reliable information about the properties of the Hubbard model. An alternative approach is to use exact diagonalization on finite clusters.

The so-called "periodic small-cluster approach" begins with the periodic crystal approximation. A bulk crystal is modeled by a lattice of M sites with periodic boundary conditions (PBC's). Bloch's theorem then labels the electron many-body wave functions by one of M k -vectors of the first Brillouin zone. The standard approach takes the thermodynamic limit ($M \rightarrow \infty$) of the noninteracting system (sampling a continuum in momentum space that spans the Brillouin zone) and treat the subsequent electron-correlation effects in an approximate manner. The small-cluster approach fixes the number of lattice sites to be small (restricting the momentum-space sampling to a coarse grid of high-symmetry points) but solves *exactly* for all electron-correlation effects. The one-electron band structure of both methods is identical when sampled at the common points in reciprocal space.

The relationship of the many-body solutions (at equal electron concentration) for the macroscopic crystal and the small cluster is much more complicated because of uncontrolled finite-size effects in the latter. However, the small-cluster approach does provide a rigorous and complementary method to study the many-body problem that may be extrapolated to macroscopic crystals.

The periodic small-cluster approach has been applied to the study of many strongly interacting model systems and real materials. It is quite successful in de-

scribing properties that depend on short-range many-body correlations. These include the heavy-fermion behavior in the Hubbard²⁰ and Anderson²¹ models, photoemission in transition metals²², alloy formation²³, surface and thin-film photoemission²⁴ in Ni and Co, surface magnetization²⁵ in Fe, as well as Hubbard and t-J models that describe high-temperature superconductivity in the CuO₂ planes²⁶.

In this thesis, an extended one-dimensional Hubbard model is first examined by means of the small-cluster approach. The model consists of a one-dimensional chain, with one fully symmetric orbital per site, an occupancy of one electron per site, one-electron hopping of strength $-t$ between nearest-neighbor sites, and two-electron interactions between electrons in the same site (U), and between electrons in neighboring sites (K).

In solving this cluster Hubbard model, group theory is used to factorize the Hamiltonian of the concerned system into block-diagonal form by using basis functions of definite spin that transform according to the irreducible representations of the full space group. The results are consistent with those of L. Milans del Bosch and L. M. Falicov²⁷.

Another cluster Hubbard model, a two-dimensional four-site square lattice cluster, is then examined in the same way. When PBC's are imposed, each site has

four first-nearest-neighbors (1NN) and four second-nearest-neighbors (2NN) respectively. Therefore, compared with one-dimensional Hubbard model, 1NN interactions must be renormalized by a factor of 2 and 2NN interactions by a factor of 4. Because only 1NN interactions are considered, the band structure of this system is basically the same as that of the previous extended one-dimensional Hubbard model (except that the 1NN hopping strength and the 1NN Coulomb interactions are all doubled) despite of the different symmetries.

Finally, a two-dimensional overlayer system is investigated in the small-cluster approach. This system consists of two overlapped four-site square lattice clusters which may consist of two different kinds of atoms. An exact solution of such an eight-site cluster with periodic boundary conditions is presented for various overlayer/substrate situations. This cluster has : (a) a single, fully symmetric orbital per site, with first-nearest-neighbor and second-nearest-neighbor hopping; (b) a Coulomb repulsion between electrons on the same site; (c) an orbital energy for the overlayer sites; (d) a nearly-half-filled band (an average occupancy of $\frac{7}{8}$ of an electron per site). Some ground-state properties of the overlayer system are reported and discussed in large- U limit.

The rest of the thesis is organized as follows. Chapter II contains the general def-

inition of Hubbard model. Chapter III explains the method of calculation (small cluster approach) and the related symmetry analysis. In Chapter IV, the applications to one-, two-dimensional clusters and the overlayer system are presented. Finally, conclusions are given in Chapter V.

CHAPTER II

The Hubbard Hamiltonian

On general grounds, the Hamiltonian of an assembly of N electrons on a given lattice can be written as

$$H = \sum_i h(\mathbf{r}_i) + \frac{1}{2} \sum_{i \neq j} \nu(\mathbf{r}_i - \mathbf{r}_j) \quad (2.1)$$

where sums run from 1 to N , and \mathbf{r}_i labels the position of the i -th electron, h is the "one-particle" part of the Hamiltonian (i.e., it contains the orbital and kinetic energy plus all the interactions with external potentials like the lattice potential and such) while ν represents the electron-electron two-body interaction.

If we choose an orthonormal basis of single-particle states $\{\phi_j\}$, by introducing creation and annihilation operators $c_{j\sigma}^\dagger$ and $c_{j\sigma}$ for electrons in state ϕ_j with spin σ ($\sigma = \uparrow$ or \downarrow), the Hamiltonian H can be rewritten in the second quantized formalism as²⁸:

$$H = \sum_{i\sigma} e_i c_{i\sigma}^\dagger c_{i\sigma} - \sum_{ij\sigma} t_{ij} c_{i\sigma}^\dagger c_{j\sigma} + \frac{1}{2} \sum_{ijkl} \sum_{\sigma\sigma'} \langle ij | \nu | kl \rangle c_{i\sigma}^\dagger c_{j\sigma'}^\dagger c_{l\sigma'} c_{k\sigma} \quad (2.2)$$

where:

$$t_{ij} \equiv t(\mathbf{R}_i - \mathbf{R}_j) = - \int d\mathbf{r} \phi_i^*(\mathbf{r}) h(\mathbf{r}) \phi_j(\mathbf{r}) = t_{ji}^* \quad (2.3)$$

$$\langle ij | \nu | kl \rangle = \int d\mathbf{r} d\mathbf{r}' \phi_i^*(\mathbf{r}) \phi_j^*(\mathbf{r}') \nu(\mathbf{r} - \mathbf{r}') \phi_k(\mathbf{r}') \phi_l(\mathbf{r}) \quad (2.4)$$

e_i is the orbital energy and \mathbf{R}_i the position vector for site i . Both h and ν have been assumed to be spin-independent (the appropriate generalizations, to include, e.g., spin-dependence, are easily done). Energies will be normalized in such a way that $t_{ii} \equiv t(0) = 0$. The following approximations will be made, which are however believed to retain the essential physics of strongly correlated electrons:

i) The orbital energy e_i is assumed to be site independent for the same kind of (equivalent) lattice sites. It will become site dependent in disordered systems, which will not be discussed in this thesis.

ii) It will be assumed that $t_{ij} \equiv t(\mathbf{R}_i - \mathbf{R}_j)$ decays fairly rapidly with the distance, so that only matrix elements between first- and second-nearest-neighbor sites need to be retained. For layered systems, both interlayer and intralayer hopping are considered although the former is believed to be substantially smaller than the latter in some cases. We will then approximate t_{ij} as:

$$t_{ij} \simeq \begin{cases} t & \text{for n.n. } \langle ij \rangle \\ s & \text{for n.n.n. } \langle ij \rangle \\ 0 & \text{otherwise} \end{cases} \quad (2.5)$$

iii) The electron-electron Coulomb interaction is assumed to be effectively screened when electrons are farther than adjacent sites apart. The dominant contributions to the Coulomb interactions will come from: $i=j=k=l$ and $j=l=i+1=k+1$; i.e., when two electrons are on the same site (U) and in neighboring sites (K). we will then approximate $\langle ij|\nu|kl \rangle$ as

$$\langle ij|\nu|kl \rangle \simeq \begin{cases} U & \text{if } i=j=k=l \\ K & \text{if } j=l=i+1=k+1 \\ 0 & \text{otherwise} \end{cases} \quad (2.6)$$

With the above approximation, the Hubbard Hamiltonian can be written as:

$$H = H_{band} + H_U + H_K \quad (2.7)$$

where

$$H_{band} = \sum_{i\sigma} e_i c_{i\sigma}^\dagger c_{i\sigma} - t \sum_{\langle ij \rangle \sigma} c_{i\sigma}^\dagger c_{j\sigma} - s \sum_{\langle ij \rangle \sigma} c_{i\sigma}^\dagger c_{j\sigma} \quad (2.8)$$

$$H_U = U \sum_i c_{i\uparrow}^\dagger c_{i\uparrow} c_{i\downarrow}^\dagger c_{i\downarrow} \quad (2.9)$$

$$H_K = K \sum_{\langle ij \rangle} c_{i\uparrow}^\dagger c_{i\uparrow} c_{j\downarrow}^\dagger c_{j\downarrow} \quad (2.10)$$

here the sum $\langle ij \rangle$ and $\langle ij \rangle$ are over 1NN and 2NN hopping.

CHAPTER III

EXACT DIAGONALIZATION METHOD

III.1 Small Cluster Approach

The small cluster approach proceeds from the promise that working with a crystal of M -atoms, with periodic boundary conditions imposed, is exactly equivalent to solving a bulk crystal, sampled at M points of the Brillouin zone. If this mini-crystal preserves the full symmetry of the lattice environment, then the sampled points will be points of high symmetry.

In the context of the many-body problem, the advantage is quite clear. In order to treat electron-electron interactions nonperturbatively, one must take into account each electronic configuration explicitly, a problem whose scope grows exponentially with the number of sites and electrons. Since the numerical solution of such a problem is in general very laborious and computationally expensive, exact results easily obtained with relatively small clusters with periodic boundary conditions are an appealing alternative for studying such a complex system.

The advantage of this sampling technique is fully realized when examining physical features that depend on the high-symmetry points of the crystal, as is often the case for electron band edges. Also, the small cluster approach can model short-range interactions quite effectively.

One of the most notable application of this method was done by Falicov and Victora¹¹ in 1984 with the solution of a four-atom tetrahedral cluster model. Dealing with this work they fully utilized group theory to factorize the Hamiltonian matrix into smaller Jordan blocks corresponding to the different irreducible representations of the underlying space group. Since then a whole series of works have been published²⁹.

III.2 Symmetry Analysis

It is well known that the dimension of the Hamiltonian matrix grows exponentially with the size of the cluster (e.g., an M -site cluster with one orbital per site has dimension $4^M \times 4^M$). Direct diagonalization of such matrices is usually very difficult even on a supercomputer. Therefore we have to simplify the system according to the symmetries inherent in the Hamiltonian and factorize the Hamiltonian matrix

into many much smaller blocks.

Being faced by the task of efficiently simplifying the Hamiltonian matrix so that it may be solved, it is clearly advantageous first to seek out any simplifications which can be made rigorously on the basis of symmetry. To assist us in the search for the full symmetry-based simplification of the Hamiltonian matrix, we draw upon the resources of group theory.

If an space operator R leaves the Hamiltonian invariant, i.e., R commutes with H , there will be no matrix elements of H between eigenstates of R corresponding to different eigenvalues for the operator R ³⁰.

The significance of this result is that, in searching for eigenfunctions that diagonalize the Hamiltonian, the search can be made separately within the classes of functions having different eigenvalues of a commuting symmetry operator since no off diagonal matrix elements of Hamiltonian will connect functions of different symmetry.

If there are several mutually commuting symmetry operators, all of which commute with Hamiltonian, we can then choose basis functions which are simultaneous eigenfunctions of all these symmetry operators. It then follows that there are no matrix elements of Hamiltonian between states which differ in their classification

according to any of the symmetry operators. Thus we may restrict our search for eigenfunctions of Hamiltonian to functions having a definite symmetry under a complete set of mutually commuting symmetry operators. In the following, we discuss several such symmetry operators to be used in the calculations.

A. Number Operator

The total-number operator $N = \sum_{i\sigma} n_{i\sigma}$ commutes with the Hamiltonian and is a conserved quantity. The many-body states may be labeled by the total number of electrons $N = N \uparrow + N \downarrow$.

B. Space Group Symmetry

Each crystal environment presents a set of symmetry operations which leaves it invariant. These operations include identity elements, operational inverses, exhibit associativity, in other words, have all the properties of a group. The spatial symmetry is labeled by the irreducible representation of the space group that transforms according to the many-body state. In our case of the Hubbard model, the space group that is symmorphic contains operations which involve both point and translational operations. The point operations consist of the various rotations and

reflections the crystal admits about a given basis point. This space group is symmetric because it consists only of point operations taken about a basis point.

To construct the character table, we can use several rules³⁰:

(1) The number of irreducible representations equals the number of classes of group elements.

(2) The dimensionalities l_i of the irreducible representations are determined by the fact that $\sum_i l_i^2 = h$. Where h is the order of the group. Since we always have the one-dimensional representation (referred to as totally symmetrical, identical) in which each group element is represented by units, we can always fill in the first row by $\chi^{(1)}(\xi_k) = 1$, where ξ_k is the k -th element of the group.

(3) The rows of the table must be orthogonal and normalized to h , with weighting factor N_k , the number of elements in ξ_k . That is

$$\sum_k \chi^{(i)*}(\xi_k) \chi^{(j)}(\xi_k) N_k = h \delta_{ij} \quad (3.1)$$

(4) The columns of the table must be orthogonal vectors normalized to $\frac{h}{N_k}$. That is

$$\sum_i \chi^{(i)*}(\xi_k) \chi^{(i)}(\xi_l) = \frac{h}{N_k} \delta_{kl} \quad (3.2)$$

(5) Elements within the i th row are related by

$$N_j \chi^{(i)}(\xi_j) N_k \chi^{(i)}(\xi_k) = l_i \sum_l c_{jkl} N_l \chi^{(i)}(\xi_l) \quad (3.3)$$

where c_{jkl} are the constants defined by the expression governing class multiplication.

Now, we can select basis functions for different irreducible representations. Let a basis function belonging to the k th row of the j th irreducible representation be denoted by $\varphi_k^{(j)}$. Then by definition the result of operation with any element of the group on $\varphi_k^{(j)}$ can be expressed as a linear combination of $\varphi_k^{(j)}$ and its partners as follows,

$$P_k \varphi_k^{(j)} = \sum_{\lambda=1}^{l_j} \varphi_{\lambda}^{(j)} \Gamma^{(j)}(R)_{\lambda k} \quad (3.4)$$

where l_j is the dimensionality of the representation. Now, if we multiply through by $\Gamma^{(i)*}(R)_{\lambda' k'}$, sum over R , and use the great orthogonality theorem³⁰ $\sum_R \Gamma^{(i)*}(R)_{\mu\nu} \Gamma^{(j)}(R)_{\alpha\beta} = \frac{h}{l_j} \delta_{ij} \delta_{\mu\alpha} \delta_{\nu\beta}$, we obtain

$$\sum_R \Gamma^{(i)*}(R)_{\lambda' k'} P_R \varphi_k^{(j)} = \frac{h}{l_j} \delta_{ij} \delta_{k k'} \varphi_{\lambda'}^{(j)} \quad (3.5)$$

From this equation we conclude that application of the operator

$$\varrho_{\lambda k}^{(j)} = \frac{l_j}{h} \sum_R \Gamma^{(j)*}(R)_{\lambda k} P_R \quad (3.6)$$

to a basis function has the property of yielding zero unless the function being operated on belongs to kth row of $\Gamma^{(j)}$. Moreover, we see that, if this condition is satisfied then the result of the operation is $\varphi_\lambda^{(j)}$. This gives us a prescription for generating all the partners of any given basis function. Also, if we set $\lambda = k$, we obtain $\varrho_{kk}^{(j)} \varphi_k^{(j)} = \varphi_k^{(j)}$ i.e., $\varphi_k^{(j)}$ is an eigenfunction of $\varrho_{kk}^{(j)}$ with eigenvalue unity. This property serves to identify uniquely the labels of any basis function. Also, since $\varrho_{kk}^{(j)}$ is a linear operator, any linear combination of functions belonging to the kth row of $\Gamma^{(j)}$ (but coming from different choices of basis functions) such as $a\varphi_k^{(j)} + b\psi_k^{(j)}$ will also belong to that row and representation.

Assuming that function $f_k^{(j)}$ belongs to the kth row of the jth irreducible representation, and F is an arbitrary function in the space. By acting a projection operator $\varrho_{kk}^{(j)}$ (Defined in Eq.(3.6)) on the function F, we can project out $f_k^{(j)}$:

$$\varrho_{kk}^{(j)} F = f_k^{(j)} \quad (3.7)$$

which after normalization is a suitable basis function $\varphi_k^{(j)}$, then use of the transfer operators $\varrho_{\lambda k}^{(j)}$ yields all its partners, since $\varrho_{\lambda k}^{(j)} \varphi_k^{(j)} = \varphi_\lambda^{(j)}$.

However, for multi-dimension representations, there is a little difference³¹:

let V be an operator which is left invariant by all the operations of group G and

let $(f_{\mu'}^{j'}, Vg_{\mu}^j)$ represent the quantum mechanical matrix element of V with respect to the two functions, f and g , with the indicated symmetry indices, then

$$(a) (f_{\mu'}^{j'}, Vg_{\mu}^j) = 0 \quad \text{if } j \neq j' \text{ or } \mu \neq \mu'$$

$$(b) \text{ if } j = j' \text{ and } \mu = \mu' \text{ the result is independent of } \mu.$$

Thus there is no matrix element of V between functions of different symmetry indices. Since all functions in j th representation are degenerate, we can use only the first element of every character matrix when projection is applied. This theorem and the fact that functions of different symmetry are orthogonal provide the entire incentive to use symmetrized functions in the projections. They assure us of a good measure of diagonalization at the very outset.

C. Spin Symmetry

The electronic states can be further characterized by their spin symmetries³⁰. Since the total spin, the total z-component of spin, and the total spin raising and lowering operators all commute with the Hamiltonian, the many-body states may be labeled by the total spin S and the total z component of spin m_s , with every state in a given spin multiplet degenerate in energy.

Since all the models we consider are of bases of singly degenerate spherically symmetric orbitals, i.e., s-orbital like, the angular momentum of the many-body functions are pure spin, with no orbital angular momentum coming into play. The total z component of spin $S_z = \frac{1}{2}(N \uparrow - N \downarrow)$ formed from the difference of these number operators, satisfies

$$S_z \psi_A = \sum_i (m_s^i) \psi_A = M_s \psi_A \quad (3.8)$$

the raising and lowering operators $S_+ = \sum_i c_{i\uparrow}^\dagger c_{i\downarrow}$ and $S_- = (S_+)^\dagger$ satisfy:

$$S_\pm \psi(m_s^1, m_s^2, \dots) = \sum_i \left[\frac{3}{4} - m_s^i(m_s^i \pm 1) \right]^{\frac{1}{2}} \psi(m_s^1 \pm 1, m_s^2 \pm 1, \dots) \quad (3.9)$$

the only nonzero value of $[\frac{3}{4} - m_s^i(m_s^i \pm 1)]$ is 1. This occurs when $m_s^i = \mp \frac{1}{2}$. Those ψ'_s which are formally generated but are inconsistent with the Pauli principle because of double occupancy of a spin-orbital function will vanish because of the antisymmetry of the determinants.

For total spin operator S^2 :

$$\begin{aligned} S^2 \psi(m_s^1, m_s^2, \dots) = & \left(\frac{3N}{4} + 2 \sum_{i>j} m_s^i m_s^j \right) \psi(m_s^1, m_s^2, \dots) \\ & + \sum_{i \neq j} \left[\frac{3}{4} - m_s^i(m_s^i + 1) \right]^{\frac{1}{2}} \left[\frac{3}{4} - m_s^j(m_s^j - 1) \right]^{\frac{1}{2}} \end{aligned}$$

$$\times \psi(m_s^i + 1, \dots, m_s^j - 1, \dots) \quad (3.10)$$

we can simplify the first term by noting that

$$\begin{aligned} 2 \sum_{i>j} m_s^i m_s^j &= \sum_i m_s^i \sum_{j \neq i} m_s^j = \sum_i m_s^i (M_S - m_s^i) \\ &= M_S^2 - \sum_i (m_s^i)^2 = M_S^2 - \frac{N}{4} \end{aligned} \quad (3.11)$$

thus the first coefficient is $M_S^2 + \frac{N}{2}$. Since the only nonzero value for the square roots is unity, the second term also can be simplified.

If any spatial orbital is occupied by two electrons with paired spins, it appears in the second term with spins reversed, which produces just a sign change because of the antisymmetry. This term cancels the contributions in the first term of all paired spins. This leaves us with the result

$$S^2 \psi_A = (M_S^2 + \frac{\text{number of unpaired spins}}{2}) \psi_A + \sum \psi'_A \quad (3.12)$$

where ψ'_A are all the determinants which differ from ψ_A by a single interchange of spin orientations between distinct spatial orbitals.

CHAPTER IV

APPLICATIONS

IV.1. An Extended One-dimensional Hubbard Model

In this section, an extended one-dimensional Hubbard model is examined by means of the small-crystal approach. The model consists of a very large (infinite) one-dimensional chain of sites i separated by a distance a . There is one s orbital per site. We choose a cluster of four sites and apply the periodic boundary conditions (see FIG.1(a)).

The Hamiltonian of such a system consists of three terms²⁷:

$$H = H_{band} + H_U + H_K \quad (4.1)$$

where

$$H_{band} = -t \sum_{i\sigma} (c_{i\sigma}^\dagger c_{i+1,\sigma} + c_{i\sigma}^\dagger c_{i-1,\sigma}) \quad (4.2)$$

$$H_U = U \sum_i c_{i\uparrow}^\dagger c_{i\uparrow} c_{i\downarrow}^\dagger c_{i\downarrow} \quad (4.3)$$

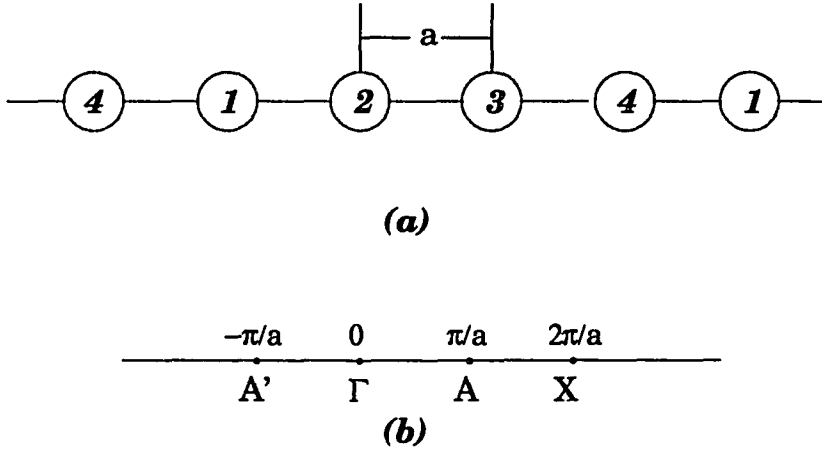


FIG.1. An extended one-dimensional cluster with PBC's in
 (a) real and (b) reciprocal space. The four symmetry stars are:
 $\Gamma(0)$, $X(\frac{2\pi}{a})$, $A(\frac{\pi}{a})$, and $A'(-\frac{\pi}{a})$.

$$H_K = K \sum_{i\sigma\sigma'} c_{i\sigma}^\dagger c_{i\sigma} c_{i+1,\sigma'}^\dagger c_{i+1,\sigma'} \quad (4.4)$$

These terms are the following: (a) a band "hopping" term between nearest-neighbor sites, with transfer integral $-t$; (b) an on-site(intra-atomic) interaction of strength U ; and (c) a nearest-neighbor(inter-atomic) interaction of strength K . Only an average occupancy of one electron per site is considered in this work. The orbital energy has been chosen as the energy reference with $e = 0$.

The system has one-dimensional translational invariance, and consequently a Brillouin zone which extends over the interval $-\frac{\pi}{a} \leq k \leq \frac{\pi}{a}$.

We consider the chain with a 4-site period. From Bloch theorem and the periodic boundary conditions, the four points sampled in k -space are (FIG.1(b)):

$$\begin{aligned} k &= 0, & \text{point } \Gamma \\ k &= \frac{\pi}{a}, & \text{point } X \\ k &= \pm \frac{\pi}{2a}, & \text{points } A, A' \end{aligned}$$

Group-theoretical analysis of the cluster and electron spin symmetry yields nine possible symmetries, corresponding to space representations Γ , X , and $A(A')$, and total spin $S=0$ (spin singlets), $S=1$ (spin triplets), and $S=2$ (spin quintets). The degeneracies of these representations are shown in Table 4.1.1.

Table 4.1.1. Degeneracy of the various representations

	Γ	X	A
S=0	1	1	2
S=1	3	3	6
S=2	5	5	10

This system has a total of $c_4^8 = \frac{8!}{4!4!} = 70$ states: 6 for S=0, 48 for S=1, and 16 for S=2. As an example, the state ($\uparrow 00 \uparrow$), which corresponds to S=0, means two double occupancies of electrons on sites 1 and 4 and nothing on sites 2 and 3.

Considering a group of translational operations $\{P_E, P_1, P_2, P_3\}$ with P_E being the identity operation, P_1 translating by a , P_2 translating by $2a$, and P_3 translating by $3a$, we can get the character table as shown in Table 4.1.2.

Table 4.1.2. The character table for the one-dimensional cluster

	P_E	P_1	P_2	P_3
Γ	1	1	1	1
X	1	-1	1	-1
A	1	i	-1	-i
A'	1	-i	-1	i

From the character table, We can produce the space symmetry projection operations ρ^i as:

$$\wp_{\Gamma} = \frac{1}{4}(P_E + P_1 + P_2 + P_3) \quad (4.5)$$

$$\wp_X = \frac{1}{4}(P_E - P_1 + P_2 - P_3) \quad (4.6)$$

$$\wp_A = \frac{1}{2}(P_E - P_2) \quad (4.7)$$

$$\wp_{A'} = \frac{1}{2}(P_1 - P_3) \quad (4.8)$$

The representation A and A' are degenerate due to time-reversal symmetry, we have taken the liner combination of the two representations to derive the equations (4.7) and (4.8) so that the coefficients are all integral real numbers. This scheme will be particularly useful for larger systems calculated on computers. To find out the eigenstates of the system, we should find out all the eigenstates of total spin S^2 first according to the principle:

$$S^2\psi_A = (M_S^2 + \frac{\text{number of unpaired spins}}{2})\psi_A + \sum \psi'_A$$

where ψ'_A are all the determinants which differ from ψ_A by a single interchange of spin orientations between distinct spatial orbitals.

For example:

$$S = 0 : S^2(\uparrow\uparrow 00) = 0$$

$$S^2((\uparrow\uparrow\downarrow 0) - (\uparrow\downarrow\uparrow 0)) = 0$$

$$S = 1 : S^2((\uparrow\uparrow\downarrow 0) + (\uparrow\downarrow\uparrow 0)) = 2((\uparrow\uparrow\downarrow 0) + (\uparrow\downarrow\uparrow 0))$$

$$S = 2 : S^2(\uparrow\uparrow\uparrow\uparrow) = 6(\uparrow\uparrow\uparrow\uparrow)$$

the above states all satisfy $S^2\psi = S(S+1)\psi$, and therefore are all eigenstates of total spin S^2 .

Now we can choose the basis functions from those 70 states for various representations and project them further, by applying the projection operators ρ^i , to get the eigenfunctions of the system which will be acted upon by the Hamiltonian.

i) $S=0$:

The basis functions are: $(\uparrow\uparrow 00), (\uparrow\uparrow 0\downarrow) - (\uparrow\downarrow 0\uparrow)$, and

$$(\uparrow\uparrow\downarrow 0) - (\uparrow\downarrow\uparrow 0) + (\uparrow 0\downarrow\uparrow) - (\uparrow 0\uparrow\downarrow).$$

For $^1\Gamma$ (the superscript is $(2S_z + 1)$, same below):

By applying ρ^F to these basis statefunctions, after normalization, we can get six eigenfunctions

$$|1\rangle = \frac{1}{2}((\uparrow\uparrow 00) + (0\uparrow\uparrow 0) + (00\uparrow\uparrow) + (\uparrow 00\uparrow))$$

$$|2\rangle = \frac{1}{4}((\uparrow\uparrow\downarrow 0) - (\uparrow\downarrow\uparrow 0) + (\uparrow 0\downarrow\uparrow) - (\downarrow 0\uparrow\uparrow))$$

$$\begin{aligned}
& +(\mathbf{0} \uparrow \downarrow \uparrow) - (\mathbf{0} \downarrow \uparrow \uparrow) + (\uparrow \downarrow \mathbf{0} \uparrow) - (\downarrow \uparrow \mathbf{0} \uparrow) \\
& +(\uparrow \mathbf{0} \uparrow \downarrow) - (\uparrow \mathbf{0} \downarrow \uparrow) + (\uparrow \uparrow \downarrow \mathbf{0}) - (\uparrow \downarrow \uparrow \mathbf{0}) \\
& +(\mathbf{0} \uparrow \uparrow \downarrow) - (\mathbf{0} \downarrow \uparrow \uparrow) + (\uparrow \uparrow \mathbf{0} \downarrow) - (\downarrow \uparrow \mathbf{0} \uparrow)
\end{aligned}$$

$$|3\rangle = \frac{1}{\sqrt{2}}((\uparrow \mathbf{0} \uparrow) + (\mathbf{0} \downarrow \mathbf{0} \uparrow))$$

$$|4\rangle = \frac{1}{2}((\uparrow \uparrow \downarrow \downarrow) + (\downarrow \downarrow \uparrow \uparrow) - (\uparrow \downarrow \downarrow \uparrow) - (\downarrow \uparrow \uparrow \downarrow))$$

$$\begin{aligned}
|5\rangle = \frac{1}{2\sqrt{2}}((\uparrow \uparrow \mathbf{0} \downarrow) - (\uparrow \downarrow \mathbf{0} \uparrow) + (\uparrow \uparrow \downarrow \mathbf{0}) - (\downarrow \uparrow \uparrow \mathbf{0}) \\
+ (\mathbf{0} \uparrow \uparrow \downarrow) - (\mathbf{0} \downarrow \uparrow \uparrow) + (\uparrow \mathbf{0} \downarrow \uparrow) - (\downarrow \mathbf{0} \uparrow \uparrow))
\end{aligned}$$

$$\begin{aligned}
|6\rangle = \frac{1}{4}((\uparrow \uparrow \downarrow \mathbf{0}) - (\uparrow \downarrow \uparrow \mathbf{0}) + (\uparrow \mathbf{0} \downarrow \uparrow) - (\uparrow \mathbf{0} \uparrow \downarrow) \\
+ (\mathbf{0} \uparrow \uparrow \downarrow) - (\mathbf{0} \downarrow \uparrow \uparrow) + (\downarrow \uparrow \mathbf{0} \uparrow) - (\uparrow \downarrow \mathbf{0} \downarrow) \\
+ (\uparrow \mathbf{0} \uparrow \downarrow) - (\downarrow \mathbf{0} \uparrow \uparrow) + (\downarrow \uparrow \uparrow \mathbf{0}) - (\uparrow \downarrow \uparrow \mathbf{0}) \\
+ (\uparrow \downarrow \mathbf{0} \uparrow) - (\downarrow \uparrow \mathbf{0} \downarrow) + (\mathbf{0} \downarrow \uparrow \uparrow) - (\mathbf{0} \uparrow \downarrow \uparrow))
\end{aligned}$$

The corresponding Hamiltonian matrix is shown in Table 4.1.3.

Table 4.1.3. The Hamiltonian matrix for $^1\Gamma$ symmetry.

$2U+4K$	$-2t$	0	0	0	0
$-2t$	$U+3K$	$-2\sqrt{2}t$	$-2t$	0	0
0	$-2\sqrt{2}t$	$2U$	0	0	0
0	$-2t$	0	$4K$	0	0
0	0	0	0	$U+4K$	0
0	0	0	0	0	$U+3K$

Similarly, we can get the eigenfunctions of the Hamiltonian and the correspondent matrices for X and $A(A')$.

For 1X :

The eigenfunctions are

$$|1\rangle = \frac{1}{2}((\uparrow\uparrow 00) - (0 \uparrow\uparrow 0) + (00 \uparrow\uparrow) - (\uparrow 00 \uparrow))$$

$$|2\rangle = \frac{1}{4}((\downarrow\uparrow\uparrow 0) - (\uparrow\downarrow\uparrow 0) + (\uparrow 0 \uparrow\uparrow) - (\downarrow 0 \uparrow\uparrow)$$

$$+ (0 \uparrow\downarrow\uparrow) - (0 \downarrow\uparrow\uparrow) + (\downarrow\uparrow 0 \uparrow) - (\uparrow\downarrow 0 \uparrow)$$

$$+ (\uparrow\uparrow\downarrow 0) - (\uparrow\downarrow\uparrow 0) + (\uparrow 0 \downarrow\uparrow) - (\uparrow 0 \uparrow\downarrow)$$

$$+ (\uparrow\uparrow 0 \downarrow) - (\downarrow\uparrow 0 \uparrow) + (0 \downarrow\uparrow\uparrow) - (0 \uparrow\uparrow\downarrow))$$

$$|3\rangle = \frac{1}{2\sqrt{3}}((\uparrow\downarrow\downarrow\uparrow) + (\downarrow\uparrow\uparrow\downarrow) + (\uparrow\uparrow\downarrow\downarrow) + (\downarrow\downarrow\uparrow\uparrow)$$

$$- 2(\uparrow\downarrow\uparrow\downarrow) - 2(\downarrow\uparrow\downarrow\uparrow))$$

$$|4\rangle = \frac{1}{2\sqrt{2}}((\uparrow\uparrow 0 \downarrow) - (\uparrow\downarrow 0 \uparrow) + (\downarrow\uparrow\uparrow) - (\uparrow\uparrow\downarrow 0))$$

$$\begin{aligned}
& +(0 \uparrow \downarrow \downarrow) - (0 \downarrow \downarrow \uparrow) + (\downarrow 0 \uparrow \downarrow) - (\uparrow 0 \downarrow \downarrow) \\
|5\rangle = & \frac{1}{4}((\uparrow \downarrow \downarrow) - (\downarrow \downarrow \uparrow) + (\uparrow 0 \downarrow \downarrow) - (\downarrow 0 \downarrow \uparrow) \\
& + (\uparrow \downarrow \downarrow 0) - (\downarrow \downarrow \downarrow 0) + (\downarrow 0 \uparrow \downarrow) - (\downarrow 0 \downarrow \uparrow) \\
& + (0 \downarrow \downarrow \uparrow) - (0 \downarrow \uparrow \downarrow) + (\downarrow \uparrow 0 \downarrow) - (\uparrow \downarrow 0 \downarrow) \\
& + (\downarrow \downarrow 0 \uparrow) - (\uparrow \downarrow 0 \downarrow) + (0 \downarrow \downarrow \uparrow) - (0 \uparrow \downarrow \downarrow)) \\
|6\rangle = & \frac{1}{\sqrt{2}}((\downarrow 0 \uparrow 0) - (0 \downarrow 0 \uparrow))
\end{aligned}$$

The corresponding Hamiltonian matrix is shown in Table 4.1.4.

Table 4.1.4. The Hamiltonian matrix for 1X symmetry.

$2U+4K$	$-2t$	0	0	0	0
$-2t$	$U+3K$	$-2\sqrt{3}t$	0	0	0
0	$-2\sqrt{3}t$	$4K$	0	0	0
0	0	0	$U+4K$	$-2\sqrt{2}t$	0
0	0	0	$-2\sqrt{2}t$	$U+3K$	$-2\sqrt{2}t$
0	0	0	0	$-2\sqrt{2}t$	$2U$

For $^1A(^1A')$:

The eigenfunctions are

$$\begin{aligned}
|1\rangle = & \frac{1}{\sqrt{2}}((\uparrow \downarrow \uparrow 00) - (00 \uparrow \downarrow)) \\
|2\rangle = & \frac{1}{2\sqrt{2}}((\uparrow \downarrow \downarrow 0) - (\downarrow \downarrow \uparrow 0) + (\uparrow \downarrow 0 \downarrow) - (\downarrow \downarrow 0 \uparrow) \\
& + (0 \downarrow \uparrow \downarrow) - (0 \uparrow \downarrow \downarrow) + (\downarrow 0 \uparrow \downarrow) - (\uparrow 0 \downarrow \downarrow))
\end{aligned}$$

$$|3\rangle = \frac{1}{2}((\uparrow\uparrow 0 \downarrow) - (\downarrow\downarrow 0 \uparrow) + (0 \downarrow\uparrow\uparrow) - (0 \uparrow\downarrow\downarrow))$$

$$\begin{aligned} |4\rangle = & \frac{1}{4}((\uparrow\uparrow\downarrow 0) - (\downarrow\downarrow\uparrow 0) + (\downarrow\downarrow 0 \uparrow) - (\uparrow\uparrow 0 \downarrow) \\ & + (0 \uparrow\downarrow\downarrow) - (0 \downarrow\uparrow\uparrow) + (\downarrow 0 \uparrow\uparrow) - (\uparrow 0 \downarrow\downarrow) \\ & + (\downarrow\uparrow\downarrow 0) - (\uparrow\downarrow\downarrow 0) + (\downarrow\uparrow 0 \downarrow) - (\uparrow\downarrow 0 \downarrow) \\ & + (\downarrow 0 \uparrow\downarrow) - (\uparrow 0 \downarrow\uparrow) + (0 \uparrow\uparrow\downarrow) - (0 \downarrow\downarrow\uparrow)) \end{aligned}$$

The corresponding Hamiltonian matrix is shown in Table 4.1.5.

Table 4.1.5. The Hamiltonian matrix for 1A symmetry.

$2U+4K$	$-2t$	0	0
$-2t$	$U+3K$	0	0
0	0	$U+4K$	$-2t$
0	0	$-2t$	$U+3K$

ii) $S=1$:

For $^3\Gamma$:

The eigenfunctions are:

$$|1\rangle = \frac{1}{2}((\uparrow\uparrow\downarrow 0) + (0 \downarrow\uparrow\uparrow) - (\uparrow 0 \downarrow\uparrow) + (\uparrow\uparrow 0 \downarrow))$$

$$|2\rangle = \frac{1}{2}((\uparrow\downarrow\uparrow\uparrow) + (\uparrow\uparrow\uparrow\downarrow) - (\uparrow\uparrow\downarrow\uparrow) - (\downarrow\uparrow\uparrow\uparrow))$$

$$|3\rangle = \frac{1}{2}((\uparrow\uparrow 0 \uparrow) + (\uparrow 0 \uparrow\downarrow) - (\uparrow\uparrow\uparrow) - (0 \uparrow\downarrow\uparrow))$$

$$|4\rangle = \frac{1}{2}((\downarrow 0 \uparrow\uparrow) + (\uparrow\uparrow\downarrow) + (0 \uparrow\uparrow\downarrow) - (\uparrow\downarrow 0 \uparrow))$$

The corresponding Hamiltonian matrix is shown in Table 4.1.6.

Table 4.1.6. The Hamiltonian matrix for ${}^3\Gamma$ symmetry.

$U+3K$	$-2t$	$-2t$	0
$-2t$	$4K$	0	$-2t$
$-2t$	0	$U+4K$	$-2t$
0	$-2t$	$-2t$	$U+3K$

For 3X :

The eigenfunctions are:

$$|1\rangle = \frac{1}{2}((\uparrow\uparrow\uparrow 0) - (0 \uparrow\uparrow\uparrow) - (\uparrow 0 \uparrow\uparrow) - (\uparrow\uparrow 0 \uparrow))$$

$$|2\rangle = \frac{1}{2}((\uparrow\uparrow 0 \uparrow) + (\uparrow\uparrow\uparrow 0) - (0 \uparrow\uparrow\uparrow) - (\uparrow 0 \uparrow\uparrow))$$

$$|3\rangle = \frac{1}{2\sqrt{2}}((\uparrow\uparrow\downarrow 0) + (\uparrow\downarrow\uparrow 0) - (0 \uparrow\uparrow\downarrow) - (0 \uparrow\downarrow\uparrow) \\ - (\downarrow 0 \uparrow\uparrow) - (\uparrow 0 \uparrow\downarrow) - (\uparrow\downarrow 0 \uparrow) - (\downarrow\uparrow 0 \uparrow))$$

The corresponding Hamiltonian matrix is shown in Table 4.1.7.

Table 4.1.7. The Hamiltonian matrix for 3X symmetry.

$U+3K$	0	0
0	$U+4K$	0
0	0	$U+3K$

For 3A :

The four eigenfunctions are:

$$|1\rangle = \frac{1}{\sqrt{2}}((\uparrow\uparrow\uparrow 0) + (\uparrow 0 \uparrow\uparrow))$$

$$|2\rangle = \frac{1}{\sqrt{2}}((\uparrow\uparrow\uparrow\downarrow) - (\uparrow\downarrow\uparrow\uparrow))$$

$$|3\rangle = \frac{1}{\sqrt{2}}((0 \uparrow\uparrow\uparrow) + (\uparrow\uparrow 0 \uparrow))$$

$$|4\rangle = \frac{1}{\sqrt{2}}((\uparrow\uparrow 0 \uparrow) + (0 \uparrow\uparrow\downarrow))$$

The corresponding Hamiltonian matrix is shown in Table 4.1.8.

Table 4.1.8. The Hamiltonian matrix for 3A symmetry.

$U+3K$	$-t$	$-t$	0
$-t$	$4K$	0	$-t$
$-t$	0	$U+4K$	t
0	$-t$	t	$U+3K$

iii) $S=2$:

Only states with 5X symmetry survives:

$$|0\rangle = (\uparrow\uparrow\uparrow\uparrow)$$

$$H|0\rangle = 4K|0\rangle \text{ with } E = 4K$$

We know from above calculations that the 70 states of this cluster are arranged in no more than 28 symmetry-required energy levels. The distribution of those levels among the nine possible symmetries is shown in Table 4.1.9. It should be emphasized that these levels are dictated by the symmetry of the problem, and that in some cases the Hubbard model, for general interactions, shows additional(accidental) degeneracies, i.e., the number of levels for this cluster may be, in general, less than 28. For specific values of the parameters the degeneracy is indeed greater. In particular, for $U=K=0$, the noninteracting limit shows a sixfold degenerate ground state of energy($-4t$) on symmetries $^3\Gamma$, $^1\Gamma$, and 1X and the number of levels reduces to five(see Table 4.1.10). In the extreme strong-interaction limit($t=0$), there are also five levels(see Table 4.1.11), with further reductions in very special cases(e.g., $U=K$, $U=0$, and $K=0$).

Table 4.1.9. The Multiplicity of the matrices for the various representations.

	Γ	X	A
$S=0$	6	6	4
$S=1$	4	3	4
$S=2$	0	1	0

Table 4.1.10. The 28 energy levels in the limit $U=K=0$.

Energy	Degeneracy	$^3\Gamma$	$^1\Gamma$	5X	3X	1X	3A	1A
-4t	6	1	1	0	0	2	0	0
-2t	16	0	0	0	0	0	2	2
0	26	2	4	1	3	2	0	0
2t	16	0	0	0	0	0	2	2
4t	6	1	1	0	0	2	0	0

Table 4.1.11. The 28 energy levels in the limit $t=0$.

Energy	Degeneracy	$^3\Gamma$	$^1\Gamma$	5X	3X	1X	3A	1A
4K	16	1	1	1	0	1	1	0
U+3K	32	2	2	0	2	2	2	2
U+4K	16	1	1	0	1	1	1	1
2U+4K	4	0	1	0	0	1	0	1
2U	2	0	1	0	0	1	0	0

IV.2. A Two-dimensional Square Lattice Cluster Hubbard Model

In this section, we study a two-dimensional four-site square lattice cluster Hubbard model. The lattice sites of the isolated cluster lie on the corners of a square and are numbered 1-4 in a counterclockwise direction(see FIG.2(a)). When PBC's are imposed, the four first-nearest neighbors (1NN) of site 1 are two each of the

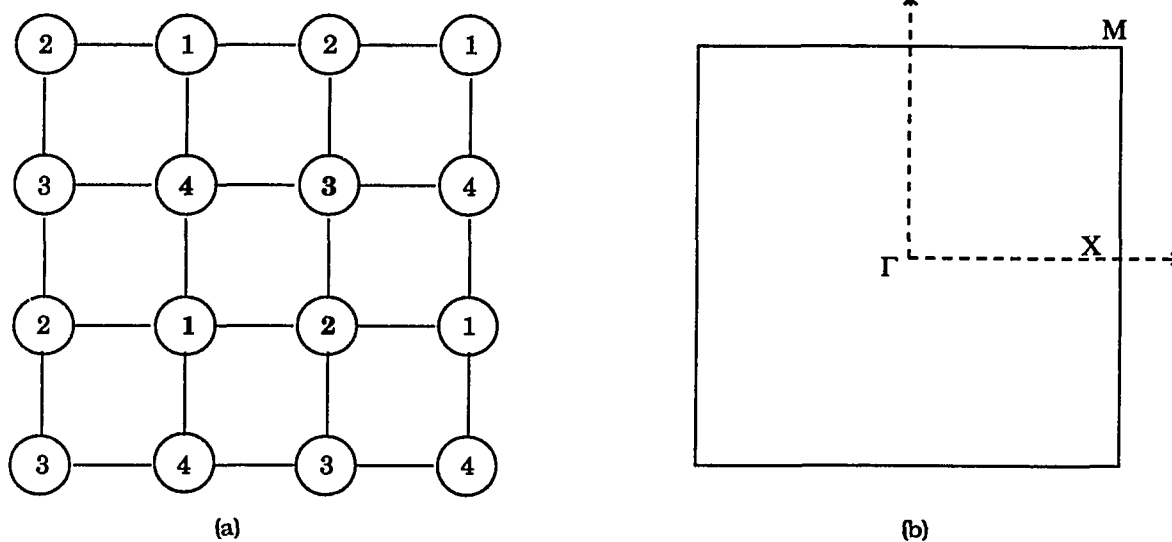


FIG.2. A four-site cluster with PBC's for the square lattice in (a) real and (b) reciprocal space. The three symmetry stars are: $\Gamma(0,0)$, $M(\frac{\pi}{a}, \frac{\pi}{a})$, $X(\frac{\pi}{a}, 0)$.

sites 2 and 4 and the four second-nearest neighbors (2NN) are four each of the site 3 (see Table 4.2.1). Therefore, 1NN interactions must be renormalized by a factor of 2 and 2NN interactions by a factor of 4 when the sum in the Hamiltonian is restricted to the sites in the cluster. Note that the imposition of PBC's does not add any new connections to the lattice. For this self-contained cluster, i.e., the cluster-permutation contained cluster, the cluster-permutation group is isomorphic to the point group c_{4v} with the origin at the site 1. The space group is of order-32 and is composed of 14 classes. The Brillouin zone is sampled at three symmetry stars: $\Gamma(d=1)$, $M(d=1)$, and $X(d=2)$.

It is easy to see that the twofold rotation $\{c_4^2|0\}$, and the reflections about the x and y axes $\{\sigma_x|0\}$ and $\{\sigma_y|0\}$, are all redundant operations; i.e., they are identical to the identity operation $\{E|0\}$ because the four-site cluster is self-contained. This implies that only irreducible representations of the space group that represent the twofold rotation and the reflections about the x and y axes by the unit matrix are acceptable representations. For a more detailed discussion, see Ref.³².

Table 4.2.1. Neighbor structure for the four-site square lattice cluster.

Site	1NN				2NN			
1	2	2	4	4	3	3	3	3
2	1	1	3	3	4	4	4	4
3	2	2	4	4	1	1	1	1
4	1	1	3	3	2	2	2	2

The character table of the full space group is recorded in Table 4.2.2. The acceptable representations are Γ_1, Γ_3 (renamed to Γ_2 in the reduced character table 4.2.4), M_1, M_2 , and X_1 .

The cluster-permutation group, with all repeated operations eliminated, is isomorphic to the point group c_{4v} (of order 8) with its origin at the site 1. Table 4.2.3 shows the mapping between the space-group notation and the point-group notation for the group elements. After rearrangement, the character table is now shown in Table 4.2.4.

There are also 70 states for this cluster: 20 for $S=0$; 45 for $S=1$; and 5 for $S=2$. The 28 symmetry-required energy levels are distributed among the 15 possible symmetries(see Table 4.2.5).

Table 4.2.3 Repeated operations of the space group for the four-site cluster in the square lattice and their identification with point-group operations. The cluster-permutation group is isomorphic to the point group C_{4v} with an origin at the center of the square. The space-group operations are denoted in the standard notation of a point-group operation followed by a translation all enclosed in curly braces. Put in more mathematical terms, this table explicitly lists the homomorphism that maps the space group onto the cluster-permutation group. The first row (corresponding to the redundant operations of the space group) forms the kernel of the homomorphism.

Point-group operation	Space-group operations		
E	$\{E 0\},$	$\{C_4^2 0\},$	$\{\sigma 0\}$
C_4^2	$\{E \theta\},$	$\{C_4^2 \theta\},$	$\{\sigma \theta\}$
C_4	$\{C_4 \tau\},$	$\{\sigma' \tau\},$	
σ	$\{E \tau\}$	$\{C_4^2 \tau\},$	$\{\sigma \tau\}$
σ'	$\{C_4 0,\theta\},$	$\{\sigma' 0,\theta\}$	

Table 4.2.4. Reduced character table for four-site square cluster.

	ξ_1	ξ_2	$2\xi_3$	$2\xi_4$	$2\xi_5$
Γ_1	1	1	1	1	1
Γ_2	1	1	-1	1	-1
M_1	1	1	-1	-1	1
M_2	1	1	1	-1	-1
X	2	-2	0	0	0

Table 4.2.5. Sizes of the Hamiltonian matrix blocks of spin and various spatial representations.

	Γ_1	Γ_2	M_1	M_2	X
S=0	5	3	3	1	4
S=1	1	2	1	3	4
S=2	0	1	0	0	0

If we consider only the first-nearest-neighbor interaction, the Hamiltonian of such a system consists of three terms:

$$H = H_{band} + H_U + H_K \quad (4.9)$$

with

$$H_{band} = -2t \sum_{(ij)\sigma} c_{i\sigma}^\dagger c_{j\sigma} \quad (4.10)$$

$$H_U = U \sum_i c_{i\uparrow}^\dagger c_{i\uparrow} c_{i\downarrow}^\dagger c_{i\downarrow} \quad (4.11)$$

$$H_K = 2K \sum_{(ij)\sigma\sigma'} c_{i\sigma}^\dagger c_{i\sigma} c_{j,\sigma'}^\dagger c_{j,\sigma'} \quad (4.12)$$

The eigenfunctions and Hamiltonian matrices belonging to states with definite spatial and spin symmetries are obtained in the same way as those described in IV.1. The results are summarized below.

For $S=0$:

$(1)^1\Gamma_1$:

The eigenfunctions are:

$$|1\rangle = \frac{1}{2}((\uparrow\downarrow\uparrow\uparrow 00) + (0\uparrow\downarrow\uparrow 0) + (00\uparrow\downarrow) + (\uparrow\uparrow 00\downarrow))$$

$$\begin{aligned} |2\rangle = & \frac{1}{4}((\uparrow\downarrow\uparrow\downarrow 0) + (\uparrow\uparrow 0\downarrow) + (0\uparrow\downarrow\uparrow) + (\uparrow\downarrow 0\downarrow) \\ & + (\uparrow\downarrow\uparrow) + (\uparrow\uparrow 0\downarrow) + (0\uparrow\downarrow) + (\uparrow\downarrow 0\uparrow) \\ & - (\uparrow\downarrow\uparrow 0) - (\uparrow\uparrow 0\downarrow) - (0\uparrow\downarrow) - (\uparrow\downarrow 0\uparrow) \\ & - (\uparrow\downarrow\uparrow 0) - (\uparrow\uparrow 0\downarrow) - (0\uparrow\downarrow) - (\uparrow\downarrow 0\uparrow)) \end{aligned}$$

$$|3\rangle = \frac{1}{\sqrt{2}}((\uparrow\uparrow 0\downarrow) + (0\uparrow\downarrow))$$

$$|4\rangle = \frac{1}{2}((\uparrow\uparrow\downarrow\downarrow) + (\downarrow\downarrow\uparrow\uparrow) - (\uparrow\downarrow\downarrow\uparrow) - (\downarrow\uparrow\uparrow\downarrow))$$

$$\begin{aligned} |5\rangle = & \frac{1}{2\sqrt{2}}((\uparrow\uparrow 0\downarrow) - (\uparrow\downarrow 0\uparrow) + (\uparrow\uparrow 0\downarrow) - (\downarrow\uparrow 0\uparrow)) \\ & + (\uparrow\downarrow\uparrow 0) - (\downarrow\uparrow\uparrow 0) + (0\uparrow\downarrow) - (0\downarrow\uparrow) \end{aligned}$$

$$\begin{aligned} |6\rangle = & \frac{1}{4}((\uparrow\downarrow\uparrow\downarrow 0) - (\uparrow\downarrow\uparrow 0) + (\uparrow\uparrow 0\downarrow) - (\uparrow\uparrow 0\downarrow) \\ & + (0\uparrow\downarrow) - (0\downarrow\uparrow) + (\downarrow\uparrow 0\uparrow) - (\uparrow\downarrow 0\downarrow) \\ & + (\uparrow\uparrow 0\downarrow) - (\downarrow\uparrow 0\uparrow) + (\downarrow\uparrow\downarrow) - (\uparrow\downarrow\downarrow 0) \\ & + (\uparrow\downarrow 0\uparrow) - (\uparrow\uparrow 0\downarrow) + (0\downarrow\uparrow) - (0\uparrow\downarrow)) \end{aligned}$$

The corresponding Hamiltonian matrix is shown in Table 4.2.6.

Table 4.2.6. The Hamiltonian matrix for ${}^1\Gamma_1$ symmetry.

$2U+8K$	$-4t$	0	0	0	0
$-4t$	$U+6K$	$-4\sqrt{2}t$	$-4t$	0	0
0	$-4\sqrt{2}t$	$2U$	0	0	0
0	$-4t$	0	$U+8K$	0	0
0	0	0	0	$U+8K$	0
0	0	0	0	0	$U+6K$

$(2) {}^1\Gamma_2$:

There is no eigenfunction transforming according to ${}^1\Gamma_2$.

$(3) {}^1M_1$:

The eigenfunctions are:

$$|1\rangle = \frac{1}{2}((\uparrow\uparrow\uparrow 00) + (00\uparrow\uparrow) - (\uparrow 00\uparrow) - (0\uparrow\uparrow 0))$$

$$|2\rangle = \frac{1}{4}((\uparrow\uparrow\downarrow 0) + (\uparrow 0\downarrow\uparrow) + (\uparrow\downarrow 0\downarrow) + (0\uparrow\downarrow\uparrow)$$

$$+ (\uparrow 0\uparrow\downarrow) + (\downarrow\uparrow\uparrow 0) + (0\uparrow\downarrow\downarrow) + (\downarrow\uparrow 0\downarrow)$$

$$- (\downarrow\uparrow\uparrow 0) - (\uparrow 0\uparrow\downarrow) - (\downarrow\downarrow 0\uparrow) - (0\uparrow\uparrow\downarrow)$$

$$- (\downarrow 0\uparrow\uparrow) - (\uparrow\downarrow\uparrow 0) - (0\downarrow\uparrow\uparrow) - (\uparrow\downarrow 0\uparrow))$$

$$|3\rangle = \frac{1}{2\sqrt{3}}((\uparrow\downarrow\downarrow\uparrow) + (\downarrow\uparrow\uparrow\downarrow) + (\uparrow\uparrow\downarrow\downarrow) + (\downarrow\downarrow\uparrow\uparrow))$$

$$-2(\uparrow\downarrow\uparrow\downarrow) - 2(\downarrow\uparrow\downarrow\uparrow))$$

The corresponding Hamiltonian matrix is shown in Table 4.2.7.

Table 4.2.7. The Hamiltonian matrix for 1M_1 symmetry.

$2U+8K$	$-4t$	0
$-4t$	$U+6K$	$-4\sqrt{3}t$
0	$-4\sqrt{3}t$	$8K$

(4) 1M_2 :

The eigenfunctions are:

$$\begin{aligned}
 |1\rangle &= \frac{1}{2\sqrt{2}}((\uparrow\uparrow\downarrow\downarrow) - (\downarrow\downarrow\uparrow\uparrow) + (\downarrow\uparrow\uparrow\downarrow) - (\uparrow\downarrow\downarrow\uparrow)) \\
 &\quad + (0\uparrow\uparrow\downarrow) - (0\downarrow\downarrow\uparrow) + (\downarrow\downarrow\uparrow\uparrow) - (\uparrow\uparrow\downarrow\downarrow)) \\
 |2\rangle &= \frac{1}{4}((\uparrow\uparrow\downarrow\downarrow) - (\downarrow\downarrow\uparrow\uparrow) + (\uparrow\downarrow\uparrow\downarrow) - (\downarrow\uparrow\downarrow\uparrow)) \\
 &\quad + (\uparrow\downarrow\uparrow\downarrow) - (\downarrow\uparrow\downarrow\uparrow) + (\uparrow\downarrow\uparrow\downarrow) - (\downarrow\uparrow\downarrow\uparrow) \\
 &\quad + (0\downarrow\downarrow\uparrow) - (0\uparrow\uparrow\downarrow) + (\downarrow\uparrow\downarrow\uparrow) - (\uparrow\downarrow\uparrow\downarrow) \\
 &\quad + (\downarrow\uparrow\downarrow\uparrow) - (\uparrow\downarrow\uparrow\downarrow) + (0\downarrow\downarrow\uparrow) - (0\uparrow\uparrow\downarrow)) \\
 |3\rangle &= \frac{1}{\sqrt{2}}((\uparrow\downarrow\uparrow\downarrow) - (0\uparrow\downarrow\uparrow\downarrow))
 \end{aligned}$$

The corresponding Hamiltonian matrix is shown in Table 4.2.8.

Table 4.2.8. The Hamiltonian matrix for 1M_2 symmetry.

$U+8K$	$-4\sqrt{2}t$	0
$-4\sqrt{2}t$	$U+6K$	$-4\sqrt{2}t$
0	$-4\sqrt{2}t$	$2U$

(5) 1X :

The eigenfunctions are:

$$|1\rangle = \frac{1}{\sqrt{2}}((\uparrow\uparrow 00) - (00 \uparrow\uparrow))$$

$$|2\rangle = \frac{1}{2\sqrt{2}}((\uparrow\uparrow\downarrow 0) + (\uparrow\uparrow 0 \downarrow) + (\downarrow 0 \uparrow\uparrow) + (0 \downarrow\uparrow\uparrow) \\ - (\uparrow\downarrow\uparrow 0) - (\downarrow\uparrow 0 \uparrow) - (\uparrow 0 \uparrow\uparrow) - (0 \uparrow\downarrow\uparrow))$$

$$|3\rangle = \frac{1}{2}((\uparrow\uparrow 0 \downarrow) - (\downarrow\downarrow 0 \uparrow) + (0 \downarrow\uparrow\uparrow) - (0 \uparrow\downarrow\downarrow))$$

The corresponding Hamiltonian matrix is shown in Table 4.2.9.

Table 4.2.9. The Hamiltonian matrix for 1X symmetry.

$2U+8K$	$-4t$	0	0
$-4t$	$U+6K$	0	0
0	0	$U+8K$	$-4t$
0	0	$-4t$	$U+6K$

For $S=1$:

$(1)^3\Gamma_1$:

The eigenfunctions are:

$$\begin{aligned}
 |1\rangle &= \frac{1}{2\sqrt{2}}((\uparrow\uparrow\uparrow 0) - (0 \uparrow\uparrow\uparrow) + (\uparrow\uparrow 0 \uparrow) - (\uparrow 0 \uparrow\uparrow) \\
 &\quad - (\uparrow 0 \uparrow\uparrow) + (\uparrow\uparrow 0 \downarrow) - (\uparrow\uparrow\downarrow 0) + (0 \uparrow\uparrow\downarrow)) \\
 |2\rangle &= \frac{1}{4}((\uparrow\uparrow\downarrow 0) + (\uparrow\downarrow\uparrow 0) - (0 \downarrow\uparrow\uparrow) - (0 \uparrow\downarrow\uparrow) \\
 &\quad + (\uparrow\uparrow 0 \downarrow) + (\uparrow\downarrow 0 \uparrow) - (\downarrow 0 \uparrow\uparrow) - (\uparrow 0 \uparrow\downarrow) \\
 &\quad - (\uparrow 0 \downarrow\uparrow) - (\uparrow 0 \uparrow\downarrow) + (\uparrow\downarrow 0 \downarrow) + (\downarrow\uparrow 0 \uparrow) \\
 &\quad + (0 \uparrow\uparrow\downarrow) + (0 \uparrow\downarrow\uparrow) - (\downarrow\uparrow\uparrow 0) - (\uparrow\downarrow\downarrow 0))
 \end{aligned}$$

The corresponding Hamiltonian matrix is shown in Table 4.2.10.

Table 4.2.10. The Hamiltonian matrix for $^3\Gamma_1$ symmetry.

$U+6K$	0
0	$U+6K$

$(2)^3\Gamma_2$:

The eigenfunctions are:

$$|1\rangle = \frac{1}{2\sqrt{2}}((\uparrow\uparrow\uparrow 0) + (0 \uparrow\uparrow\uparrow) - (\uparrow\uparrow 0 \uparrow) - (\uparrow 0 \uparrow\uparrow))$$

$$+(\downarrow 0 \uparrow \uparrow) + (\uparrow \uparrow 0 \downarrow) + (0 \downarrow \uparrow \uparrow) + (\uparrow \uparrow \downarrow 0))$$

$$|2\rangle = \frac{1}{2}((\downarrow \uparrow 0 \uparrow) + (\uparrow 0 \uparrow \downarrow) - (\uparrow \downarrow \uparrow 0) - (0 \uparrow \downarrow \uparrow))$$

$$|3\rangle = \frac{1}{2}((\uparrow \downarrow \uparrow \uparrow) + (\uparrow \uparrow \uparrow \downarrow) - (\uparrow \uparrow \downarrow \uparrow) - (\downarrow \uparrow \uparrow \uparrow))$$

The corresponding Hamiltonian matrix is shown in Table 4.2.11.

Table 4.2.11. The Hamiltonian matrix for ${}^3\Gamma_2$ symmetry.

$U+6K$	$-4\sqrt{2}t$	$-4\sqrt{2}t$
$-4\sqrt{2}t$	$U+8K$	0
$-4\sqrt{2}t$	0	$8K$

$(3) {}^3M_1$:

The eigenfunctions are:

$$|1\rangle = \frac{1}{2\sqrt{2}}((\downarrow \uparrow \uparrow 0) - (0 \uparrow \uparrow \downarrow) + (\uparrow \downarrow 0 \uparrow) - (\uparrow 0 \downarrow \uparrow))$$

$$+(\downarrow 0 \uparrow \uparrow) - (\uparrow \uparrow 0 \downarrow) + (\uparrow \uparrow \downarrow 0) - (0 \downarrow \uparrow \uparrow))$$

$$|2\rangle = \frac{1}{2}((\downarrow \uparrow 0 \uparrow) - (\uparrow 0 \uparrow \downarrow) + (\uparrow \downarrow \uparrow 0) - (0 \uparrow \downarrow \uparrow))$$

The corresponding Hamiltonian matrix is shown in Table 4.2.12.

Table 4.2.12. The Hamiltonian matrix for 3M_1 symmetry.

$U+6K$	0
0	$U+8K$

$(4)^3M_2$:

There is only one eigenfunction for this representation.

$$|1\rangle = \frac{1}{2\sqrt{2}}((\uparrow\uparrow\uparrow 0) + (0 \uparrow\uparrow\downarrow) - (\uparrow\downarrow 0 \uparrow) - (\uparrow 0 \uparrow\downarrow) \\ - (\downarrow 0 \uparrow\uparrow) - (\uparrow\uparrow 0 \downarrow) - (0 \downarrow\uparrow\uparrow) - (\uparrow\uparrow\downarrow 0)) \\ H|1\rangle = (U + 6K)|1\rangle \quad \text{with} \quad E = U + 6K.$$

$(5)^3X$:

The eigenfunctions are:

$$|1\rangle = \frac{1}{\sqrt{2}}((\uparrow\uparrow\uparrow 0) + (\uparrow 0 \uparrow\downarrow)) \\ |2\rangle = \frac{1}{2}((\uparrow\uparrow 0 \uparrow) + (0 \uparrow\uparrow\downarrow) - (\uparrow\uparrow\uparrow 0) - (\uparrow 0 \uparrow\downarrow)) \\ |3\rangle = \frac{1}{2}((\uparrow\uparrow\downarrow\uparrow) + (\uparrow\uparrow\uparrow\downarrow) - (\downarrow\uparrow\uparrow\uparrow) - (\uparrow\downarrow\uparrow\uparrow)) \\ |4\rangle = \frac{1}{\sqrt{2}}((\uparrow\downarrow 0 \uparrow) + (0 \uparrow\uparrow\downarrow))$$

The corresponding Hamiltonian matrix is shown in Table 4.2.13.

Table 4.2.13. The Hamiltonian matrix for 3X_1 symmetry.

$U+6K$	$-2\sqrt{2}t$	$-2\sqrt{2}t$	0
$-2\sqrt{2}t$	$U+8K$	0	$2\sqrt{2}t$
$-2\sqrt{2}t$	0	$8K$	$-2\sqrt{2}t$
0	$2\sqrt{2}t$	$-2\sqrt{2}t$	$U+6K$

For $S=2$:

Only with 5M_1 symmetry survives in this case.

The eigenfunction for 5M_1 is

$$|1\rangle = (\uparrow\uparrow\uparrow\uparrow)$$

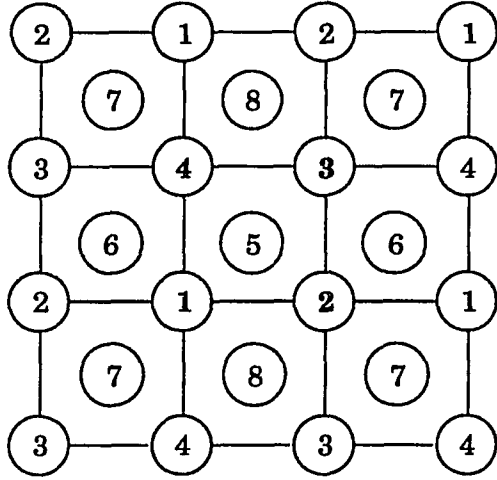
$$H|1\rangle = 8K|1\rangle, \quad \text{with} \quad E = 8K.$$

IV.3. An Overlay System

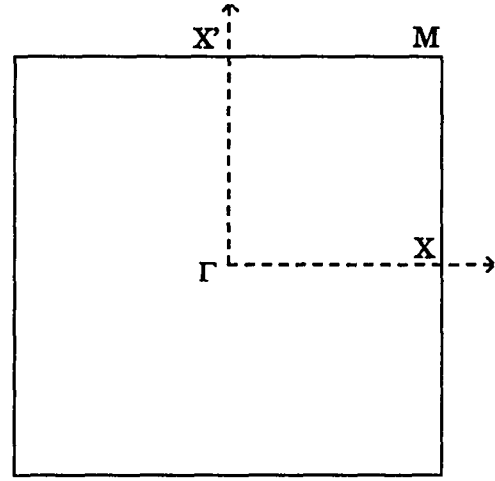
In this section, we study the property of a two-dimensional overlayer system with various overlayer/substrate situations. The overlayer cluster consists of two overlapped square lattices which may contain different kinds of atoms. The lattice sites are numbered 1-8(see FIG.3(a)). When PBC's are imposed, the four first-nearest-neighbors(1NN) of site 1 are 5-8 and the four second- nearest-neighbors (2NN) are two each of the sites 2 and 4. Table 4.3.1 presents the neighbor structure of the cluster.

Table 4.3.1. Neighbor structure for the eight-site square lattice cluster.

Site	1NN				2NN			
1	5	6	7	8	2	2	4	4
2	5	6	7	8	1	1	3	3
3	5	6	7	8	2	2	4	4
4	5	6	7	8	1	1	3	3
5	1	2	3	4	6	6	8	8
6	1	2	3	4	5	5	7	7
7	1	2	3	4	6	6	8	8
8	1	2	3	4	5	5	7	7



(a)



(b)

FIG.3. An eight-site cluster with PBC's for the square lattice in (a) real and (b) reciprocal space. The four symmetry stars are: $\Gamma(0,0)$, $M(\frac{\pi}{a}, \frac{\pi}{a})$, $X(\frac{\pi}{a}, 0)$, $X'(0, \frac{\pi}{a})$.

The Hamiltonian of such a system consists of four terms:

$$H = H_{orbital} + H_{hopping} + H_U + H_K \quad (4.13)$$

with

$$H_{orbital} = e \sum_{i\sigma(i)4} c_{i\sigma}^\dagger c_{i\sigma} \quad (4.14)$$

$$H_{hopping} = -2t \sum_{(ij)\sigma} c_{i\sigma}^\dagger c_{j\sigma} - 2s \sum_{(ij)\sigma} c_{i\sigma}^\dagger c_{j\sigma} \quad (4.15)$$

$$H_U = U_1 \sum_{i\langle 4} c_{i\uparrow}^\dagger c_{i\uparrow} c_{i\downarrow}^\dagger c_{i\downarrow} + U_2 \sum_{i\langle 4} c_{i\uparrow}^\dagger c_{i\uparrow} c_{i\downarrow}^\dagger c_{i\downarrow} \quad (4.16)$$

$$H_K = 2K \sum_{(ij)\sigma\sigma'} c_{i\sigma}^\dagger c_{i\sigma} c_{j\sigma'}^\dagger c_{j\sigma'} \quad (4.17)$$

Here the factor 2 in eqs. (4.15) and (4.17) is due to the renormalization introduced by the PBC's as discussed in IV.2. Only an average occupancy of $\frac{7}{8}$ of an electron per site is considered in this work. In the large-U limit, it corresponds to a strongly correlated system.

The point group is $G_p = \{E, C_4, C_4^2, C_4^{-1}\}$ and the translational group is $G_t = \{0, t_1, t_2, t_3\}$, with t_1, t_2 , and t_3 being the vectors pointing from site 1 toward sites 2,

4, and 3. The space group G , produced by the direct product $G_p \otimes G_t$, is of order-16 and is composed of 5 classes. The Brillouin zone is sampled at four symmetry stars: $\Gamma(d=1)$, $M(d=1)$, $X(d=2)$ and $X'(d=2)$.

This cluster has a total of $C_7^{16} = \frac{16!}{9!7!} = 11440$ states: 4707 for $S = \frac{1}{2}$; 5376 for $S = \frac{3}{2}$; 1296 for $S = \frac{5}{2}$; and 64 for $S = \frac{7}{2}$. There are 40 possible symmetries corresponding to space representations: $\Gamma_1, \Gamma_2, \Gamma_3, \Gamma_4, M_1, M_2, M_3, M_4, X_1$, and X_2 . (see Table 4.3.2.).

Table 4.3.2. Sizes of the Hamiltonian matrix blocks of spin and various spatial representations.

	Γ_1	Γ_2	Γ_3	Γ_4	M_1	M_2	M_3	M_4	X_1	X_2
$S = \frac{1}{2}$	2	0	1	1	0	0	0	0	1	1
$S = \frac{3}{2}$	14	16	15	15	24	0	24	0	27	27
$S = \frac{5}{2}$	80	80	80	80	176	0	176	0	168	168
$S = \frac{7}{2}$	156	152	154	154	280	0	280	0	294	294

Based on the rules described in Section III.2(B), we can construct the character table as shown in Table 4.3.3. From Table 4.3.2, one can see that even after the symmetry reduction, the Hamiltonian matrix blocks are still too large to be handled "manually" as in the previous cases. We use a symmetry-adapted computer algo-

rithm to generate all many-body states and perform the symmetry projectons. The result and Hamiltonian matrix blocks are then diagonalized to set both eigenvalues and eigenvectors.

Table 4.3.3. The character table for the overlayer system.

	ξ_1	ξ_2	ξ_3	ξ_4	$2\xi_5$	$2\xi_6$	$2\xi_7$	$2\xi_8$	$2\xi_9$	$2\xi_{10}$
Γ_1	1	1	1	1	1	1	1	1	1	1
Γ_2	1	1	1	1	-1	-1	1	1	-1	-1
Γ_3	1	-1	1	-1	-1	1	$-i$	i	i	$-i$
Γ_4	1	-1	1	-1	-1	1	i	$-i$	$-i$	i
M_1	1	1	1	1	1	1	-1	-1	-1	-1
M_2	1	1	1	1	-1	-1	-1	-1	1	1
M_3	1	-1	1	-1	1	-1	i	$-i$	i	$-i$
M_4	1	-1	1	-1	1	-1	$-i$	i	$-i$	i
X_1	2	2	-2	-2	0	0	0	0	0	0
X_2	2	-2	-2	2	0	0	0	0	0	0

We report some preliminary results of the application to the study of ground-state properties of the overlayer system. We vary the parameters to simulate various overlayer/substrate situations. The results are summarized below together with some discussion on underlying physics.

(1) $t=1.0$, $s=0.1$, $U_1 = U_2=10.0$, $K=0.0$, $e=0.0$.

This parameter set corresponds to a two-dimensional fcc/bcc system with intermediate interaction strength. The ground state is of symmetry $^4\Gamma_1$, i.e., a partially

saturated ferromagnetic state. It is driven by the interaction (U) term that favors singly occupied states to avoid the on-site Coulomb energy.

(2). $t=1.0$, $s=0.1$, $U_1 = U_2=10.0$, $K=3.0$, $e=0.0$.

This parameter set differs from the first one in K. The ground state is of symmetry $^2\Gamma_4$, i.e., a spin minimally aligned state. It is easy to understand: the K term drives electrons apart to avoid the energy (K) when it dominates over the U term and the electrons will be in double occupied states.

(3). $t=1.0$, $s=0.1$, $U_1 = U_2=100.0$, $K=0.0$, $e=0.0$.

This parameter set differs from the first one in U. The ground state is of symmetry $^8\Gamma_1$. The system is a strongly correlated regime. All the electrons are in singly occupied states, yielding the spin maximally aligned, i.e., saturated ferromagnetic state.

(4). $t=-1.0$, $s=-0.1$, $U_1 = U_2=100.0$, $K=0.0$, $e=0.0$.

The ground state is of symmetry $^8\Gamma_1$. The change of sign in the single-particle hopping parameters does not affect the result obtained above.

(5). $t=1.0$, $s=0.1$, $U_1=100.0$, $U_2=0.0$, $K=0.0$, $e=0.0$.

Here we set $U_2 = 0.0$. This corresponds to non-interacting overlayer sites. Electrons will reside on those sites, yielding a spin minimally aligned ground state of

symmetry ${}^2\Gamma_4$.

(6). $t=1.0, s=0.1, U_1=100.0, U_2=0.0, K=0.0, e=5.0$.

This parameter set differs from the above one by setting $e = 5.0$. The ground state is of symmetry ${}^4\Gamma_3$, i.e., a partially saturated ferromagnetic state. This is apparently caused by the energy required to put electrons on the over layer sites.

(7). $t=1.0, s=0.1, U_1=100.0, U_2=0.0, K=0.0, e=-5.0$.

The ground state is of symmetry ${}^2\Gamma_4$. In this case, the negative orbital energy on the overlayer sites further pushes the electrons to those sites, leading to the calculated spin- $\frac{1}{2}$ ground state.

(8). $t=0.1, s=1.0, U_1 = U_2=10.0, K=0.0, e=0.0$.

Now we set the overlayer/substrate (1NN) hopping strength t to be much less than the substrate/substrate (2NN) one s . We found that the ground states are of symmetries 2X_1 and 2X_2 (degenerate). Comparing with case (1), it can be seen that one-particle effects are the origin in changing the ground-state symmetry and magnetization.

(9). $t=0.1, s=1.0, U_1 = U_2=10.0, K=3.0, e=0.0$.

This parameter set differs from the previous one in the K -term. The ground states are of symmetries ${}^2\Gamma_3$ and ${}^2\Gamma_4$ (degenerate). They have the same magneti-

zation but different symmetries compared to the above case.

$$(10). \quad t=0.1, s=1.0, U_1 = U_2=100.0, K=0.0, e=0.0.$$

This parameter set is similar to that of case (8) except that the on-site interaction strengths are increased by ten times. The ground states in this situation are of symmetries ${}^4\Gamma_3$ and ${}^4\Gamma_4$ (degenerate).

$$(11). \quad t=0.1, s=-1.0, U_1 = U_2=100.0, K=0.0, e=0.0.$$

Now we set $s = -1.0$, and we found that the ground state is of symmetry ${}^4\Gamma_1$ which has the same magnetization as in the above case but different spatial symmetry.

$$(12). \quad t=0.1, s=1.0, U_1=100.0, U_2=0.0, K=0.0, e=0.0.$$

The ground state in this situation is of symmetry 2X_1 . This is similar to the case (5).

$$(13). \quad t=0.1, s=1.0, U_1=100.0, U_2=0.0, K=0.0, e=5.0.$$

Here we set $e = 5.0$. The ground state is of symmetry 2X_1 which means that the increase of the overlayer orbital energy does not affect the result obtained in the previous situation. The situation is similar to the case (6). It indicates that the non-interacting overlayer sites that accommodate two electrons per site are still dominant here.

(14). $t=0.1$, $s=1.0$, $U_1=100.0$, $U_2=0.0$, $K=0.0$, $e=-5.0$.

The ground state is of symmetry ${}^2\Gamma_1$. The situation is similar to the case (7).

CHAPTER V

Conclusions

Three Hubbard models: an extended one-dimensional, a four-site square and an eight-site overlayer cluster, have been examined in the periodic small-cluster approach. An average occupancy of one electron per site (half-filled) is considered in the first two models while the last one is considered for an average occupancy of $\frac{7}{8}$ of an electron per site (nearly-half-filled).

In the extended one-dimensional case, there are no more than 28 symmetry-allowed energy levels which are distributed among the nine possible symmetries. In the non-interacting limit ($U=K=0$), the number of levels reduces to five because of a sixfold degenerate ground state of energy with symmetries $^3\Gamma$, $^1\Gamma$, and 1X . In the extreme strong-interaction limit ($t=0$), there are also five levels because of additional degeneracies.

For the two-dimensional four-site square lattice cluster, there are also no more than 28 symmetry-required energy levels but distributed among the 15 possible symmetries. In general, the number of levels may be less than 28 because additional

degeneracies exist.

There are totally 11440 states and 40 possible symmetries for the overlayer lattice cluster. In large- U limit, the ground-state properties of the system are studied for various overlayer/substrate situations. When the overlayer/substrate (1NN) hopping strength (t) is much greater than the substrate/substrate (2NN) one (s), the ground states are partially or completely saturated ferromagnetic when no neighbor interactions exist ($K=0$) and the overlayer-site orbital energy is positive; but the system will be antiferromagnetic when K is increased or the overlayer-site orbital energy becomes negative. If, however, the overlayer/substrate (1NN) hopping strength is much less than the substrate/substrate (2NN) one, the ground states are basically antiferromagnetic and become partially ferromagnetic only when $K=0$ and $e=0$ and $U_2 \neq 0$. The change of sign in the single-particle hopping parameters does not affect the magnetization in both cases; although the ground-state symmetry may be modified.

In future work, we will use this overlayer model to study electronic, magnetic and optical properties of various models and real overlayer systems.

BIBLIOGRAPHY

1. J. Hubbard, Proc. R. Soc. London, Ser A 276, 238 (1963).
2. D.R. Penn, Phys. Rev. 142, 350 (1966).
3. D. Denley and L.M. Falicov, Phys. Rev. B17, 1289 (1978).
4. D. Adler, in *Solid State Physics*, edited by H. Ehrenreich, F. Seitz, and D. Turnbull (Academic, New York, 1968), Vol. 21, P.1.
5. N.F. Mott and Z. Zinamon, Rep. Prog. Phys. 33, 881 (1970).
6. P.W. Anderson, Science 235, 1196 (1987).
7. E.H. Lieb and F.Y. Wu, Phys. Rev. Lett. 20, 1145 (1968).
8. J.E. Hirsch, Phys. Rev. Lett. 53, 2327 (1984).
9. B. Fourcade and G. Spronken, Phys. Rev. B29, 5089, 5096 (1984).
10. K.B. Whaley and L.M. Falicov, J. Chem. Phys. 87, 7160 (1987).
11. L.M. Falicov and R.H. Victora, Phys. Rev. B 30, 1695 (1984).
12. J. Callaway, D.P. Chen, and Y. Zhang, Phys. Rev. B35, 3705 (1987).
13. J. M. Luttinger, Phys. Rev. 121, 1251 (1961).
14. P. Nozieres and J.M. Luttinger, Phys. Rev. 127, 1423 (1962).
15. M.C. Gutzwiller, Phys. Rev. a 137, 1726 (1965).

16. M. Weger and D. Fay, Phys. Rev. B 34, 5939 (1986).
17. P. Coleman, Phys. Rev. B 29, 3035 (1984).
18. J.E. Hirsch, Phys. Rev. Lett. 54, 1317 (1985).
19. D. J. Scalapino, in *High Temperature Superconductivity, The Los Alamos Symposium*, edited by K. S. Bedell et. al. (Addison-Wesley, New York, 1990).
20. A. Reich and L.M. Falicov, Phys. Rev. B 37, 5560 (1988); 38, 11199 (1988); Changfeng Chen, A. Reich, and L. M. Falicov, Phys. Rev. B 38, 12823 (1988).
21. J. Kim, J. Callaway, and D. P. Chen, Phys. Rev. B 47,(1993).
22. R.H. Victora and L.M. Falicov, Phys. Rev. Lett. 55, 1147 (1985); E.Sowa and L.M.Falicov, Phys. Rev. B35,3765(1988).
23. A. Reich and L. M. Falicov, Phys. Rev. B 36, 3117 (1987); E. Sowa and L. M. Falicov, Phys. Rev. B 37, 8707 (1988).
24. Changfeng Chen and L. M. Falicov, Phys. Rev. B40, 3560 (1990); Changfeng Chen, Phys. Rev. Lett. 64, 2176 (1990); Changfeng Chen, Phys. Rev. B41, 5031 (1990); 43, 6347 (1991); 45,13811 (1992).
25. Changfeng Chen, Phys. Rev. B 41, 1320 (1990).
26. There are numerous papers in the literature on this subject. It is impossible to include an exhaustive list here. For work on the Hubbard model see, for example, E. Dagotto, Int. J. Mod. Phys. B 5, 77 (1991); for the calculation of parameters using ab initio methods, see, for example, M. S. Hybertsen, E. B. Stechel, M. Schluter, and D. R. Jennison, Phys. Rev. B 41, 11068 (1990).

27. L. Milans del Bosch, L.M. Falicov, Phys. Rev. B 37, 6073 (1988).
28. A.P. Balachandran, E. Ercolessi, G. Morandi, A.M. Srivastava,
Hubbard Model and Anyon Superconductivity, (1990).
29. See references in L.M. Falicov, *Recent Progress in Many-body Theories*,
vol. I, edited by E. Pajanne and R. Bishop, (Plenum, New York, 1988),
P.275.
30. Michael Tinkham, *Group Theory and Quantum Mechanics*.
31. A.W. Luehrmann, Adv. in Phys., Vol. 17, No. 65 (1968).
32. J.K. Freericks, L.M. Falicov, Phys. Rev. B 44, 2895 (1991).